

Supporting Information

Hybrid phase 1T/2H-MoS₂ with controllable 1T concentration and its promoted hydrogen evolution reaction

Yuxiao Zhang,^a Yasutaka Kuwahara,^{abc} Kohsuke Mori,^{ab} Catherine Louis^d and Hiromi

*Yamashita^{*ab}*

^a Division of Materials and Manufacturing Science, Graduate School of Engineering, Osaka University, 2-1 Yamada-oka, Osaka 565-0871, Japan

^b Unit of Elements Strategy Initiative for Catalysts & Batteries (ESICB), Kyoto University, Katsura, Kyoto 565-0871, Japan

^c JST, PRESTO, 4-1-8 Hon-Cho, Kawaguchi, Saitama 332-0012, Japan

^d Sorbonne Universités, UPMC Univ Paris 06, UMR CNRS 7197, Laboratoire de Réactivité de Surface, 4 Place Jussieu, Tour 43-33, 3ème étage, Case 178, F-75252 Paris, France

Table S1 Specific surface area and total pore volume of samples synthesized under different amount of DMF precursors calculated from N₂ adsorption isotherm data.

Sample	S _{BET} (m ² g ⁻¹)	V _{total} (cm ³ g ⁻¹)
MoS ₂	55.2	0.177
1T/2H-MoS ₂ (D25)	51.8	0.238
1T/2H-MoS ₂ (D50)	31.6	0.146
1T/2H-MoS ₂ (D75)	10.6	0.039
1T/2H-MoS ₂ (D100)	28.3	0.099

Table S2 Electrochemical performances: onset overpotential (in HER), Tafel slopes (in HER), charge transfer resistance (R_{ct}) and solution resistance (R_s) of MoS_2 , 1T/2H-MoS₂ (D25), 1T/2H-MoS₂ (D50), 1T/2H-MoS₂ (D75) and 1T/2H-MoS₂ (D100).

Sample	Onset overpotential (mV)	Tafel slope (mV/dec)	R_{ct} (Ω)	R_s (Ω)
MoS_2	270.5	363.0	361.3	42.0
1T/2H-MoS ₂ (D25)	243.6	119.9	30.0	13.4
1T/2H-MoS ₂ (D50)	146.6	71.7	20.9	12.1
1T/2H-MoS ₂ (D75)	226.2	161.5	134.3	14.0
1T/2H-MoS ₂ (D100)	240.2	117.1	159.4	8.9

Table S3 Electrochemical performances: onset overpotential (in HER), Tafel slopes (in HER), charge transfer resistance (R_{ct}) and solution resistance (R_s) of MoS_2 , 1T/2H- MoS_2 (N50), 1T/2H- MoS_2 (N100), 1T/2H- MoS_2 (N200), 1T/2H- MoS_2 (N400), 1T/2H- MoS_2 (N800) and 1T/2H- MoS_2 (N1600).

Sample	Onset overpotential (mV)	Tafel slope (mV/dec)	R_{ct} (Ω)	R_s (Ω)
MoS_2	270.5	363.0	361.3	42.0
1T/2H- MoS_2 (N50)	225.1	96.8	58.9	11.3
1T/2H- MoS_2 (N100)	223.2	105.5	71.8	9.7
1T/2H- MoS_2 (N200)	214.1	66.6	95.0	10.5
1T/2H- MoS_2 (N400)	236.8	66.5	71.1	10.1
1T/2H- MoS_2 (N800)	231.1	66.6	88.6	11.8
1T/2H- MoS_2 (N1600)	264.1	241.9	289.3	12.0

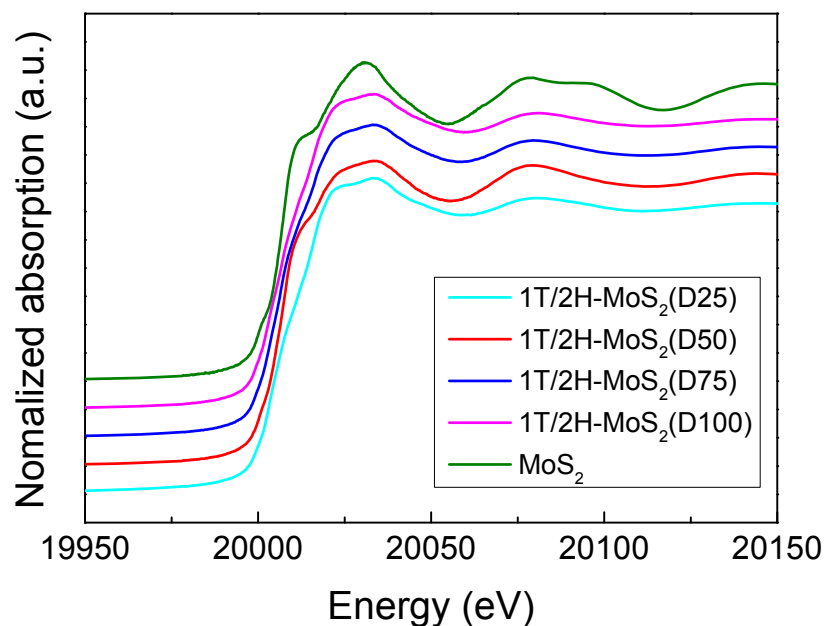


Fig. S1 XANES spectra of 1T/2H-MoS₂ (D25), 1T/2H-MoS₂ (D50), 1T/2H-MoS₂ (D75), 1T/2H-MoS₂ (D100) and MoS₂.

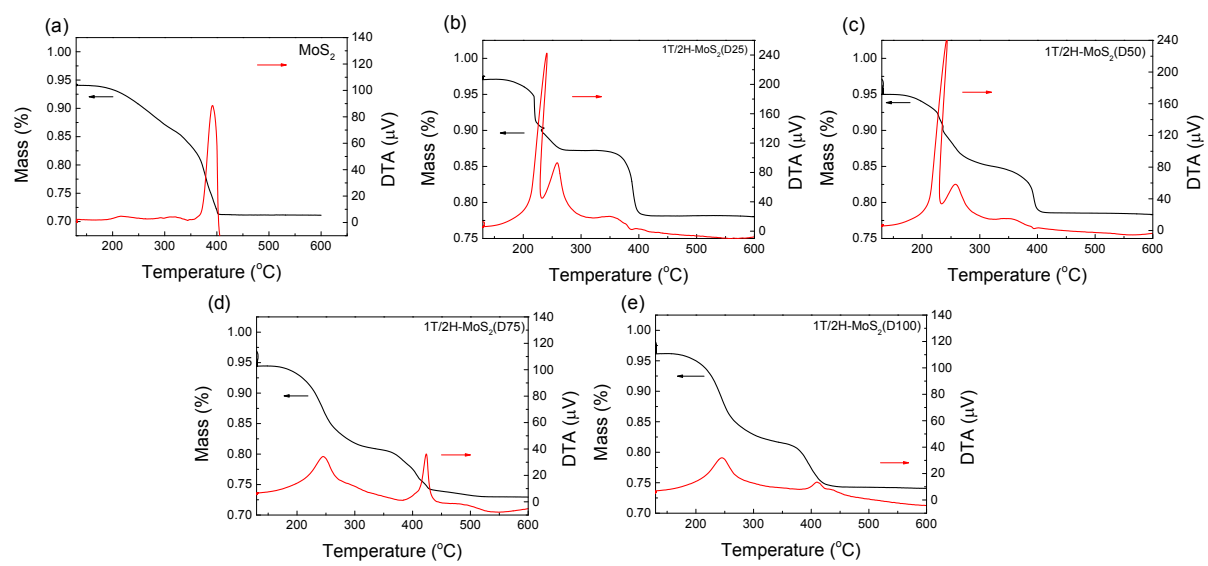


Fig. S2 TG/DTA spectra of (a) MoS₂, (b) 1T/2H-MoS₂ (D25), (c) 1T/2H-MoS₂ (D50), (d) 1T/2H-MoS₂ (D75) and (e) 1T/2H-MoS₂ (D100).

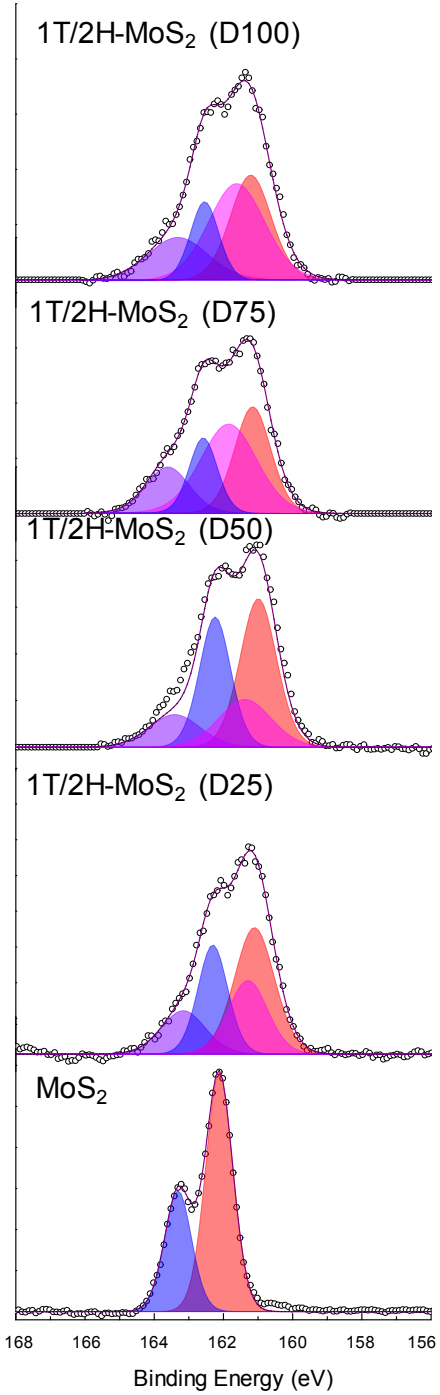


Fig. S3 S 2p XPS spectra of 1T/2H-MoS₂ (D25), 1T/2H-MoS₂ (D50), 1T/2H-MoS₂ (D75), 1T/2H-MoS₂ (D100) and MoS₂.

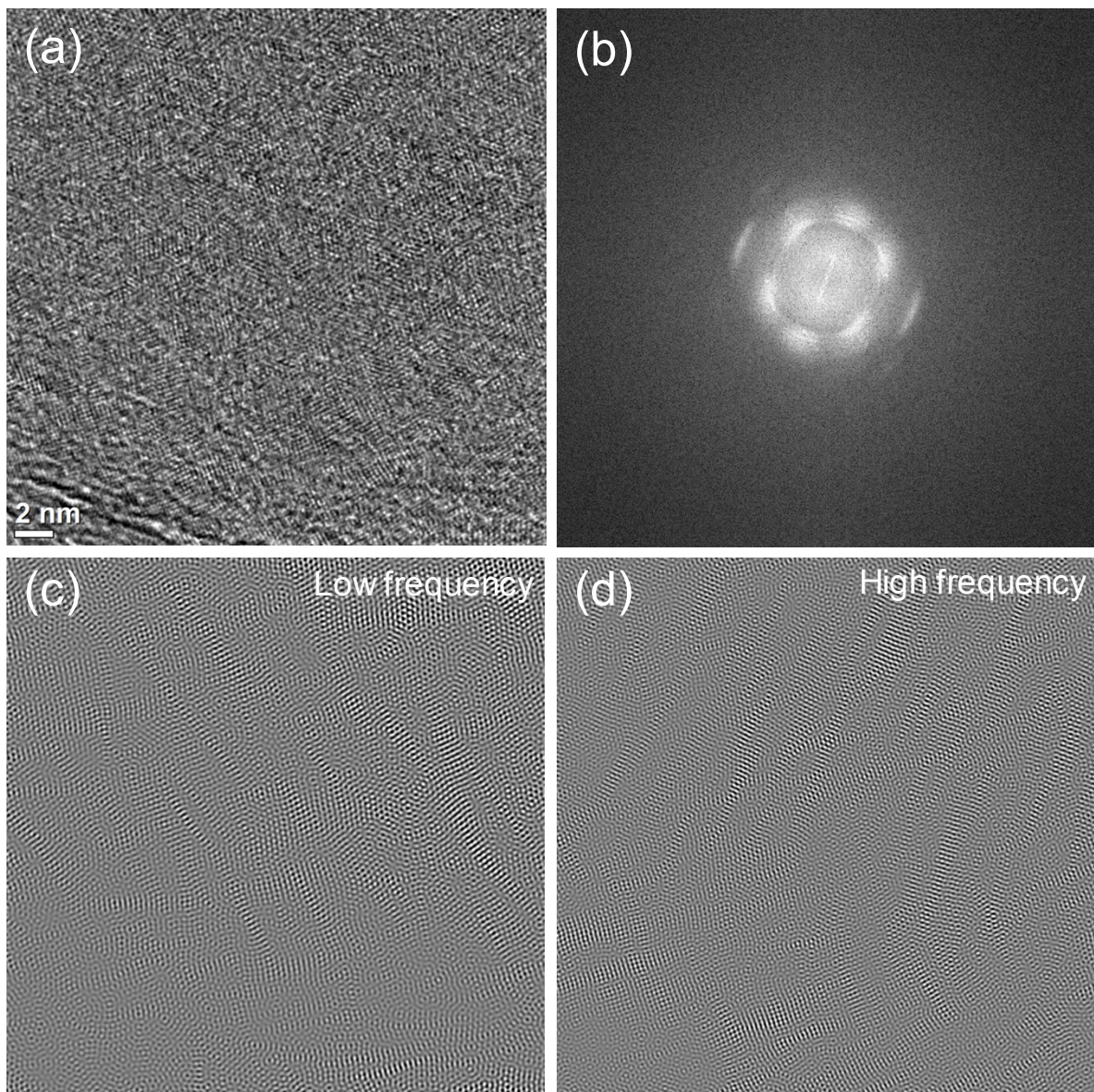


Fig. S4 (a) High-resolution TEM (HR-TEM) image of 1T/2H-MoS₂, (b) Fast Fourier transform (FFT) patterns from (a). (c), (d) inverse Fourier transform patterns under low frequency and high frequency, respectively.

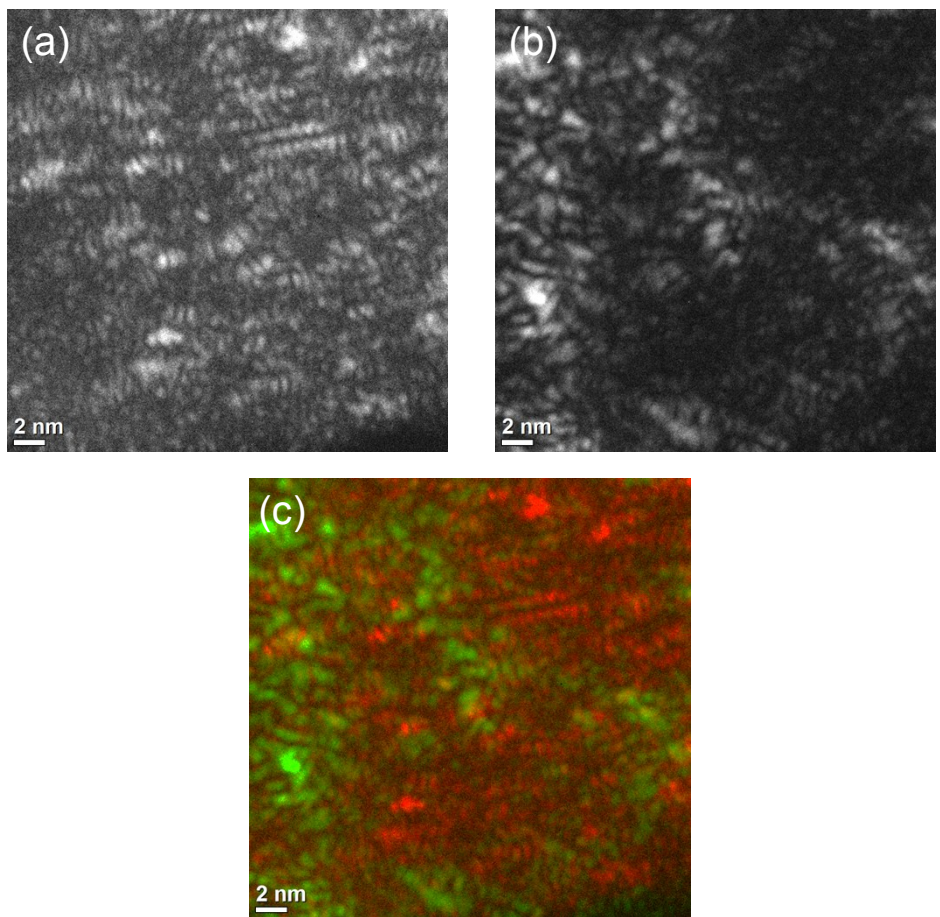


Fig. S5 Dark-field images of high-resolution TEM focused on (a) lattice spacing of 0.27 nm (2H phase), (b) lattice spacing of 0.24 nm (1T phase) and (c) mixture of two image (green: 1T, red: 2H).

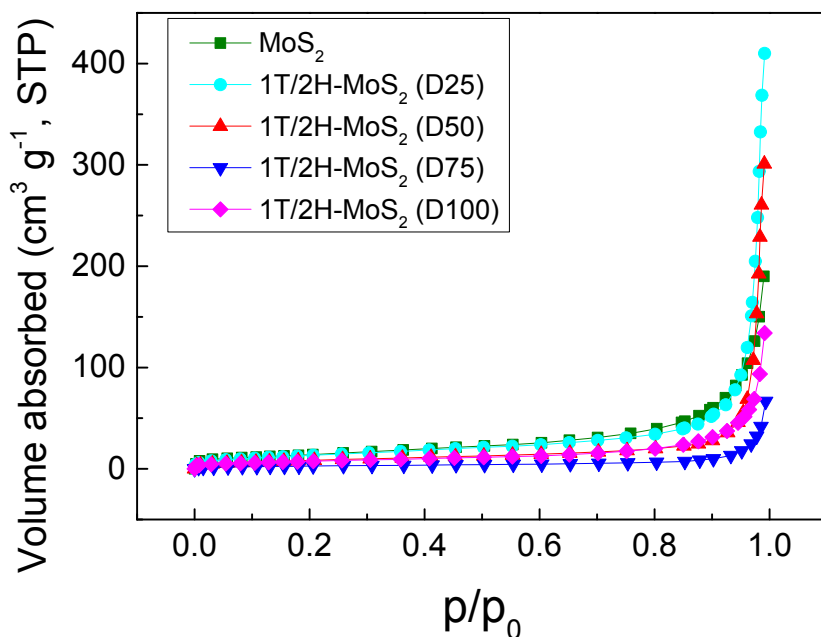


Fig. S6 N₂ adsorption-desorption isotherms of 1T/2H-MoS₂ (D25), 1T/2H-MoS₂ (D50), 1T/2H-MoS₂ (D75), 1T/2H-MoS₂ (D100) and MoS₂.

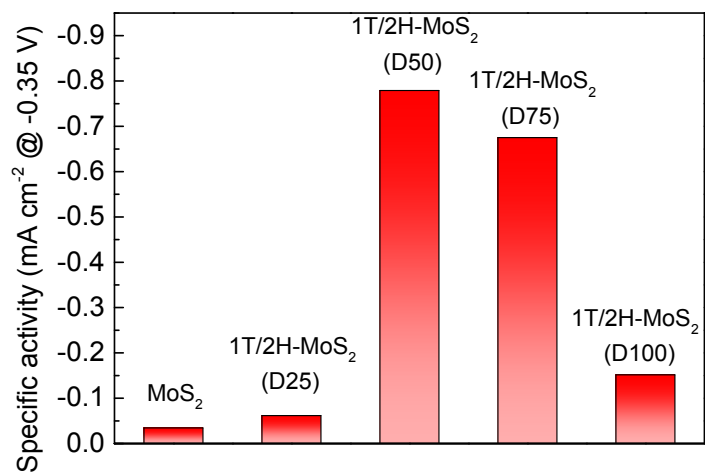


Fig. S7 Specific activity at -0.35 V of 1T/2H-MoS₂ (D25), 1T/2H-MoS₂ (D50), 1T/2H-MoS₂ (D75), 1T/2H-MoS₂ (D100) and MoS₂.

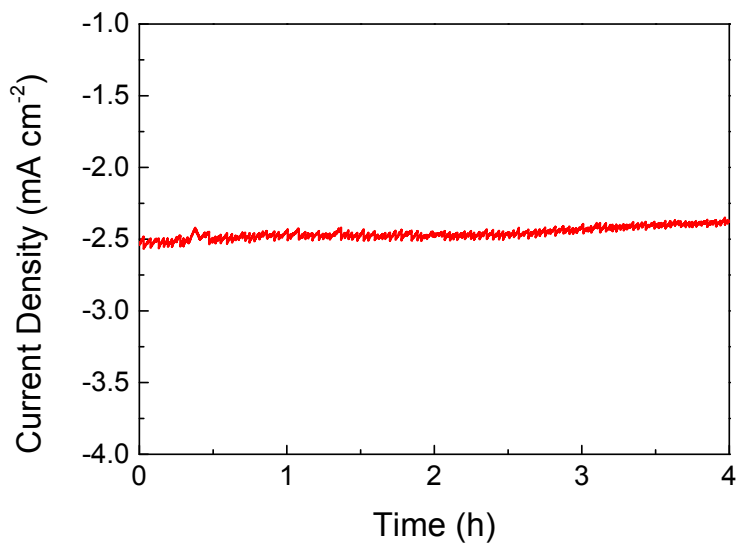


Fig. S8 I-t curve of 1T/2H-MoS₂ (D50) under overpotential of 0.3 V.

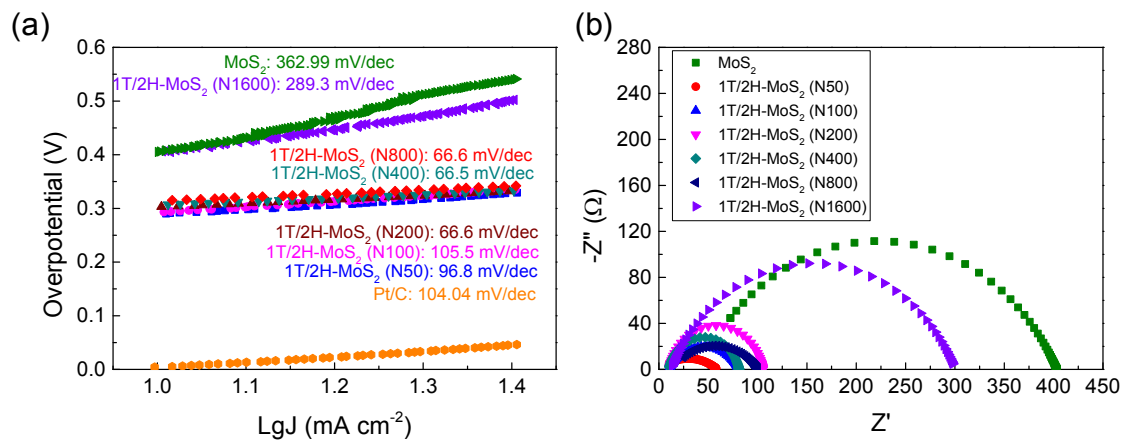


Fig. S9 (a) Tafel slopes of $1\text{T}/2\text{H}-\text{MoS}_2$ (N50), $1\text{T}/2\text{H}-\text{MoS}_2$ (N100), $1\text{T}/2\text{H}-\text{MoS}_2$ (N200), $1\text{T}/2\text{H}-\text{MoS}_2$ (N400), $1\text{T}/2\text{H}-\text{MoS}_2$ (N800), $1\text{T}/2\text{H}-\text{MoS}_2$ (N1600), MoS_2 and Pt/C. (b) Nyquist plot (fitted) of $1\text{T}/2\text{H}-\text{MoS}_2$ (N50), $1\text{T}/2\text{H}-\text{MoS}_2$ (N100), $1\text{T}/2\text{H}-\text{MoS}_2$ (N200), $1\text{T}/2\text{H}-\text{MoS}_2$ (N400), $1\text{T}/2\text{H}-\text{MoS}_2$ (N800), $1\text{T}/2\text{H}-\text{MoS}_2$ (N1600) and MoS_2 .

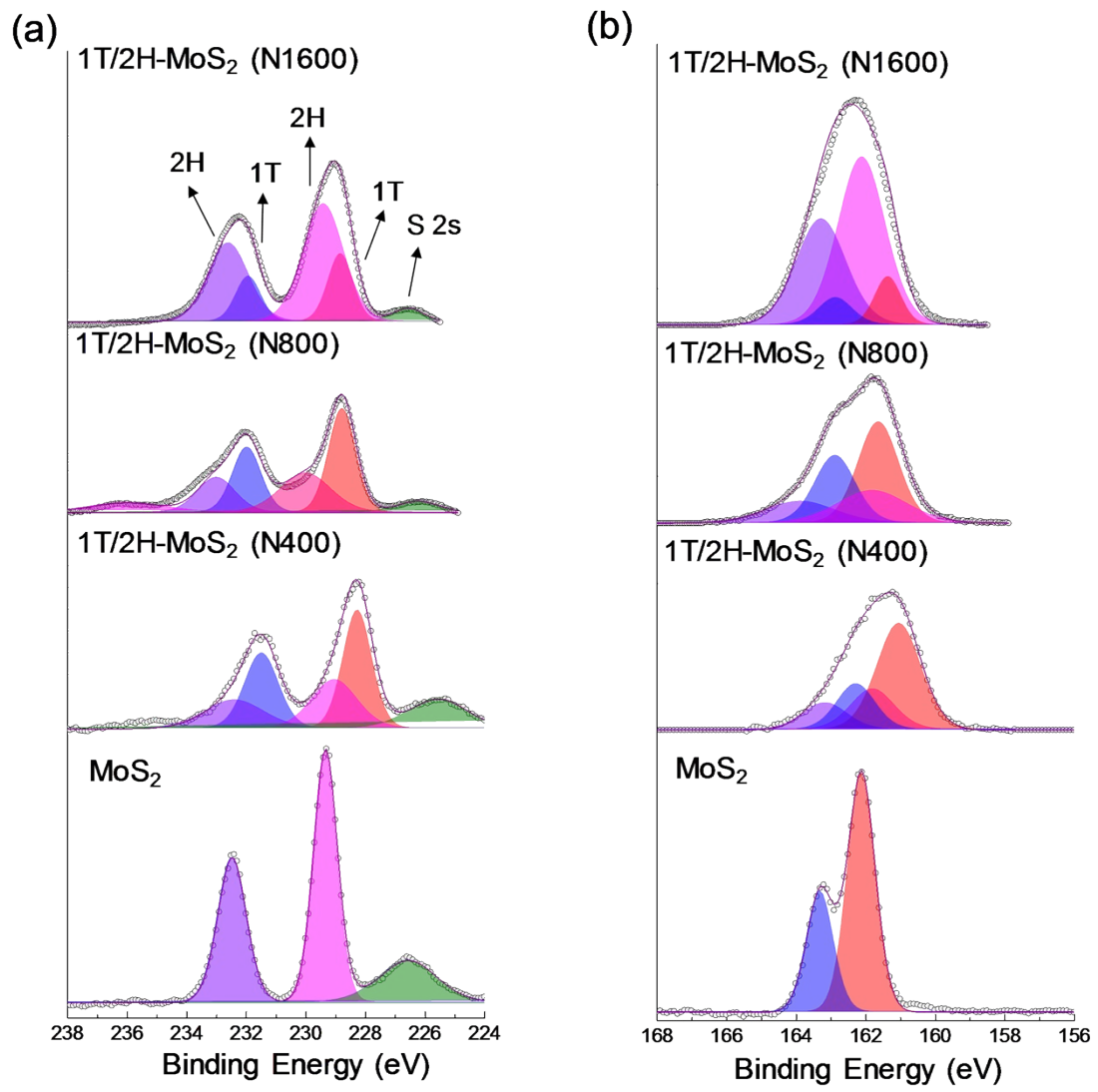


Fig. S10 (a) Mo 3d, (b) S 2p XPS spectra of 1T/2H-MoS₂ (N1600), 1T/2H-MoS₂ (N800), 1T/2H-MoS₂ (N400) and MoS₂.

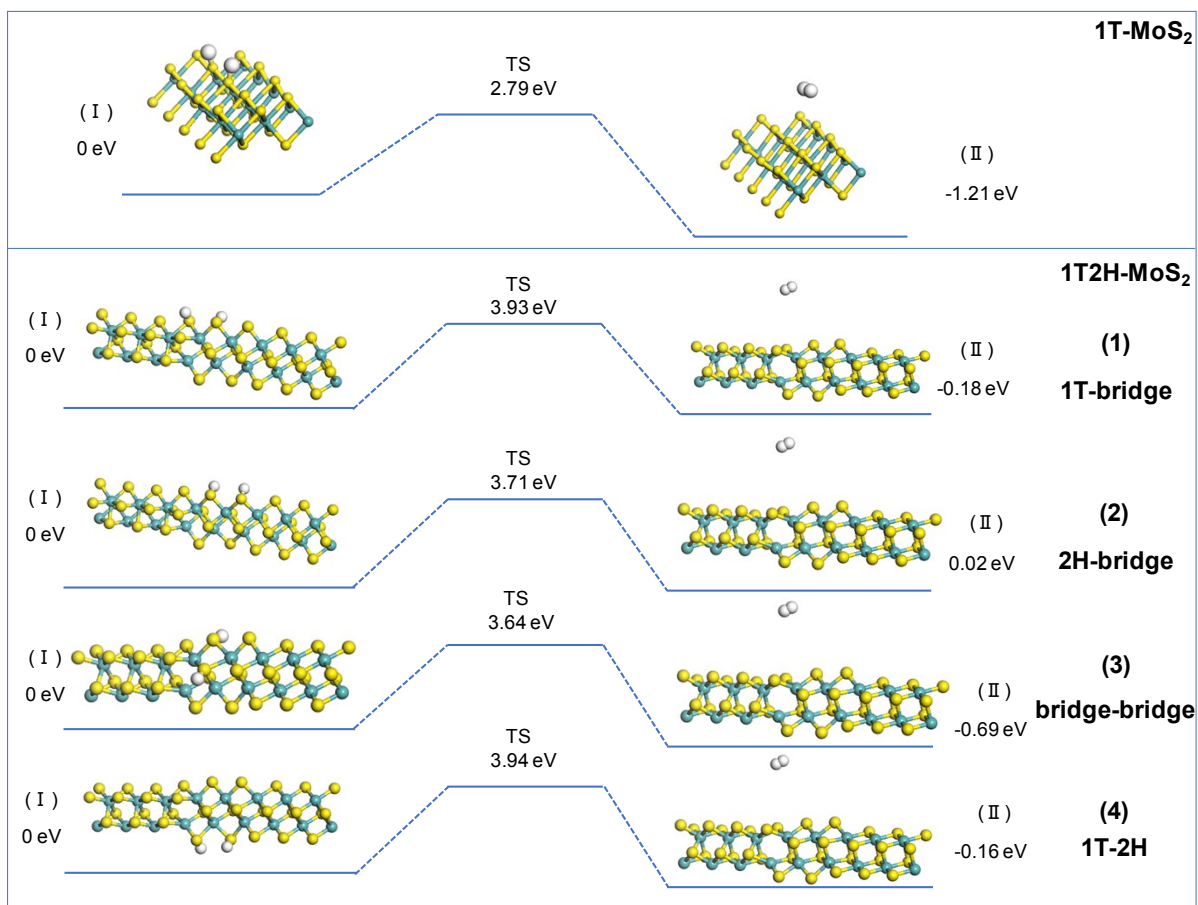


Fig. S11 Geometric structures of the initial state (I) and final state (II) of Tafel reaction and its energetics on (100)-S atoms of 1T-MoS₂ and 1T/2H interface.